XVII IMEKO World Congress
Metrology in the 3rd Millennium
June 22–27, 2003, Dubrovnik, Croatia

ON FAULT DIAGNOSIS OF ANALOGUE ELECTRONIC CIRCUITS WITH ACCESSIBILITY TO INTERNAL NODES BASED ON TRANSFORMATIONS IN MULTIDIMENSIONAL SPACES

Zbigniew Czaja, Romuald Zielonko

Gdansk University of Technology, Faculty of Electronics, Telecommunications and Informatics, Department of Electronic Measurement, ul. G. Narutowicza 11/12, 80-952 Gdansk, Poland

Abstract − In the paper new methods of fault localisation and identification in linear electronic circuits (two-port or multiport type) based on bilinear transformations in multidimensional spaces are presented. The novelty of these methods lies in transferring family of identification loci from a plane to multidimensional spaces. It implies greater distances between the loci and, in consequence, better fault resolution as well as robustness against non-faulty component tolerances and measurement errors. The methods can be used for diagnosis of electronic circuits in conventional testing systems and neural networks. They may be also useful in one or two-parameter identification measurements of other multi-parameter objects modelled by electrical circuits.

Keywords: fault localisation and identification, neural network, transformations in multidimensional spaces.

1. INTRODUCTION

In testing and fault diagnosis of analog and mixed signal electronic circuits new testing and diagnostic methods are needed. Some possibilities of synthesis and development of such methods are offered by bilinear transformation. In our previous works [1,2] input-output two-port 3D and 4D methods, based on measurement of circuit functions and mapping of loci in 3 and 4-dimensional spaces of these functions were presented.

In this paper we propose an extension of the previous input-output methods to the diagnosis of electronic circuits with some measurement access to internal nodes.

In the first part of the paper the principle of the methods in two-port version is explained on the example of 3D method for single and double fault diagnosis. Next, an extension of two-port methods to the diagnosis of circuits with accessibility to internal nodes is presented. In the last part some experimental results and implementation of the 4D and 6D methods in the neural network are included.

2. IDEA OF TWO-PORT MULTI-DIMENSIONAL METHODS

The novelty of proposed by us methods based on transformations in multi-dimensional spaces lies in transferring family of identification loci (named p_i-loci) form a plane to multi-dimensional spaces. It implies greater distances between loci and, in consequence, better fault resolution.

Here we present the 3D, 4D and 6D methods based on transformations in 3, 4 and 6-dimensional spaces in two-port version.

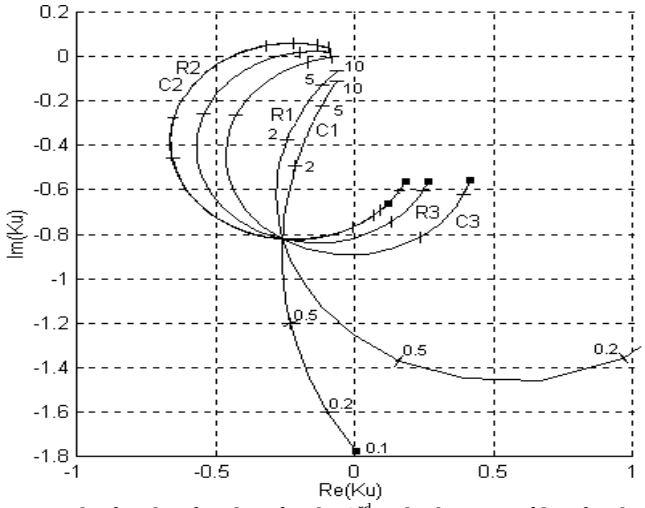

Fig 1. The family of p_i-loci for the 3rd-order low-pass filter for the 2D method based on function K_u for f_{opt}=830Hz

These methods are related to the bilinear transformation 2D method [3] based on the bilinear form of circuit function which maps changes of circuit component parameters p_i into a family of p_i-loci on a complex plane, as shown in Fig. 1. These loci can be used for localisation and identification of parametric (soft) faults via measurements of the real and the imaginary part of a single circuit function. It was difficult to implement this method in practice, because in many cases p_i-loci are situated too close to each other or superimpose one another (e.g. C_2, R_2 loci in Fig. 1).

Authors proposed the measurement of more independent circuit functions of the two-port under test (with taking into account real and imaginary parts) and imaging p_i-loci in multidimensional spaces, as shown in Fig. 2.

We will explain details of the proposed methods on the example of the 3D method for single and double fault diagnosis using a graphical approach.

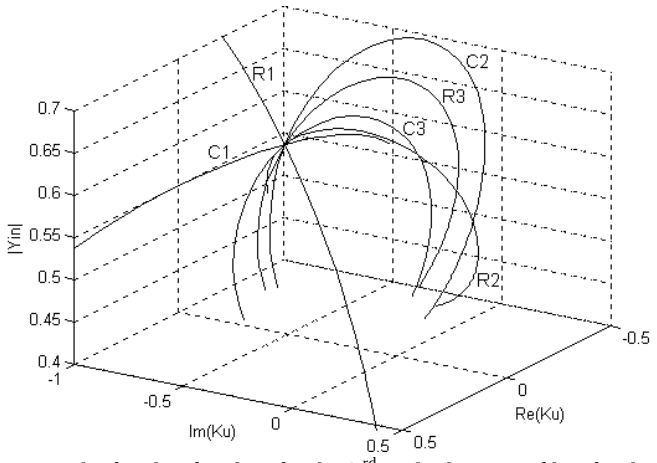

Fig 2. The family of p_i-loci for the 3 rd -order low-pass filter for the 3D method based on K_u and Y_{in} functions at f=735Hz

The starting point of the method is choosing two independent circuit functions $F^1(\cdot)$ and $F^2(\cdot)$ (for example the voltage transmittance K_u and the input admittance Y_{in}) and express them as a function of single p_i parameter or two p_i, p_l parameters functions: $F_i^1(p_i)$, $F_i^2(p_i)$ or $F_{il}^1(p_i, p_l)$, $F_{il}^2(p_i, p_l)$.

For single fault diagnosis we use the transformation:

$$T_i(p_i) = \mathrm{Re}(F_i^1(p_i))\mathbf{i} + \mathrm{Im}(F_i^1(p_i))\mathbf{j} + \left|(F_i^2(p_i))\right|\mathbf{k}, \quad (1)$$

where: **i**, **j**, **k** – are versors, $|\cdot|$ – absolute value, i=1, 2, .., N, N – the number of circuit parameters,
which maps changes of p_i-values into p_i-loci in three-dimensional space created in the system of co-ordinates $\mathrm{Re}(F_i^1(p_i))$, $\mathrm{Im}(F_i^1(p_i))$, $|(F_i^1(p_i))|$.

In Fig. 2 a family of p_i-loci obtained from the transformation (1) for 6-elements 3-order low pass filter is shown. From comparison of graphs in Fig. 1 and Fig. 2 it is clearly seen that the distances between p_i-loci in space are considerably greater than in a plane. It is also seen that C_2 and R_2-loci are separated. It is an advantage of the 3D method over the 2D one, which leads to better fault resolution and also to robustness against the influence of measurement errors and of component tolerances, which cause fuzzyfication of p_i-loci.

Results of measurement of real and imaginary parts of the first function and of the absolute value of the second one determine the measurement point $\mathrm{T_m}$ in the space (Fig. 2). The faulty element can be localised by finding the p_i-locus passing through the measurement point or nearest to it. The scale of the determined locus gives the possibility of fault identification.

For diagnosis of double faults via the 3D method the following transformation of two-parameter functions can be used:

$$T_{ij}(p_i, p_l) = \mathrm{Re}(F_{il}^1(p_i, p_l))\mathbf{i} + \mathrm{Im}(F_{il}^1(p_i, p_l))\mathbf{j} + \left|(F_{il}^2(p_i, p_l))\right|\mathbf{k} \quad (2)$$

The transformation (2) maps changes of a pair of p_i p_l -parameters into the p_i p_l-surface in 3D space. For different p_i p_l pairs we obtain a family of p_i p_l-surfaces.

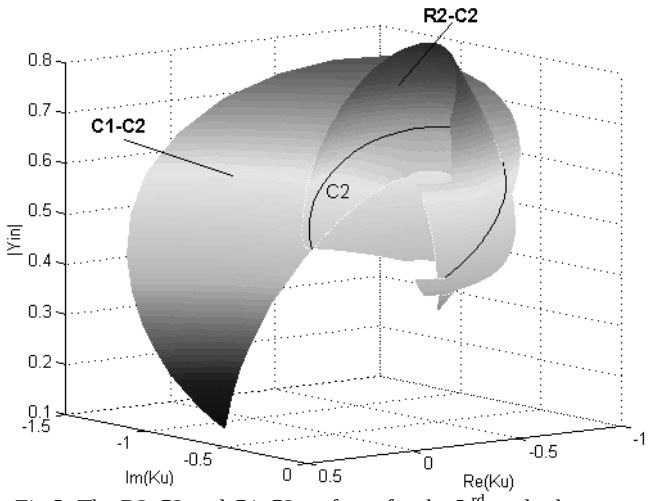

Fig 3. The R2-C2 and C1-C2 surfaces for the 3 rd -order low-pass filter for the 3D method based on K_u and Y_{in} functions at f=735Hz

An example of two surfaces for R_2 C_2 and C_1 C_2 parameters of the investigated 3-order low pass filter is shown in Fig. 3. The intersection of the surfaces represents the C_2-locus (shown in Fig. 2).

The attachment of the measuring point to the appropriate p_i p_l-surface localises the double fault. A lattice placed on the surface, scaled in p_i and p_l-values, enables identification of a double fault.

The 4D and 6D methods can be explained similarly. In these methods the distances between p_i-loci are greater with comparison to the 3D method. So, they are more effective. For example, distances between R_1-locus and C_1-locus in the point $2C_{1\ \mathrm{nom}}$ for the 3D, 4D and 6D methods are longer in comparison with the 2D method: 3.9, 5.8 and 7.7 times appropriately The 6D method can be used also for diagnosis of triple faults.

The disadvantage of the considered input-output methods is limitation to diagnosis of only two-port circuits, with a moderate number of elements (order 10). In practice (e.g. in testing via the mixed signal testing bus IEEE 1149.4), methods enabling the diagnosis of more complicated circuits with access to some internal nodes are needed. So, the goal of this paper is extending the input-output methods to the diagnosis of mentioned above circuits which can be modelled as multiports.

3. EXTENSION OF THE INPUT-OUTPUT METHODS TO MULTI-PORT DIAGNOSIS

For enabling the diagnosis of a circuit with some access to internal nodes we will use not only input-output circuit functions but also additionally internal node circuit functions (e.g. node transmittances). For simplicity, in both classes of functions we will name node functions and will note $F_i^{nj}(\cdot)$.

In the case of single fault diagnosis we propose a new transformation:

$$T_i^m(p_i) = \sum_{j=1}^{m} \left(\mathrm{Re}(F_i^{nj}(p_i)\mathbf{k}^{2j-1} + \mathrm{Im}(F_i^{nj}(p_i)\mathbf{k}^{2j}\right), \quad (3)$$

where: $F_i^{nj}(p_i)$ is the *j*-kind node circuit functions of p_i-parameter, *j*=1,2,..,*m*, *m* – the number of circuit functions, **k** – versor (unit vector).

The transformation (3) maps changes of p_i-parameters into p_i-loci in 2*m*-dimensional space.

For double fault diagnosis transformation of two-parameter node functions $F_{il}^{nj}(p_i, p_l)$ can be used:

$$T_{il}^{m}(p_i, p_l) = \sum_{j=1}^{m} \left(\mathrm{Re}(F_{il}^{nj}(p_i, p_l)\mathbf{k}^{2j-1} + \mathrm{Im}(F_{il}^{nj}(p_i, p_l)\mathbf{k}^{2j} \right), \quad (4)$$

where: $F_i^{nj}(p_i)$ is the node function of p_i and p_l parameters ($i \neq l$) and ($2 \le m$).

This transformation maps changes of a pair of $p_i p_l$-parameters into the $p_i\, p_l$-hypersurface in 2*m*-dimensional space.

It is possible to generalise (3) and (4) for multiple fault diagnosis using the transformation:

$$T_{i_1 i_2 .. i_k}^{m}(p_{i_1}, p_{i_2}, .., p_{i_k}) = \sum_{j=1}^{m} (\mathrm{Re}(F_{i_1 i_2 .. i_k}^{nj}(p_{i_1}, p_{i_2}, .., p_{i_k})\mathbf{k}^{2j-1} + \mathrm{Im}(F_{i_1 i_2 .. i_k}^{nj}(p_{i_1}, p_{i_2}, .., p_{i_k})\mathbf{k}^{2j}) \quad (5)$$

where: p_{i_1}, p_{i_2},.., p_{i_k} – circuit parameters, *k* – number of faults ($k \le 2m-1$ and $k \le N$).

The transformation (5) maps changes of a set of p_{i_1}, p_{i_2},.., p_{i_k} – parameters into *k*-dimensional hypersolid in 2*m*-dimesional space.

In a practice of most important meaning are single and double fault diagnosis and sometimes the triple fault one.

4. ALGORITHMS OF FAULT DIAGNOSIS

To explain the principles of the proposed methods we use a graphical approach, which gives the possibility to illustrate p_i-loci on the plane and in space. However, for implementation of the methods in practice, an analytical approach based on real time calculation of appropriate chosen points of p_i-loci or $p_i p_l$-surfaces from analytical formulas (written as Matlab functions) is more convenient. We will use the analytical approach in presented algorithms of soft fault localisation and identification. We assume identification of soft faults in the interval from $0.1p_{i\,nom}$ to $10p_{i\,nom}$ around the nominal point of circuit under test (CUT). We implemented all algorithms in the form of Matlab scripts.

4.1. Single fault diagnosis algorithm

The algorithm searches all p_i-loci and finds a locus lying nearest to the measurement point and determines the p_{iS}-value with minimum distance to this point. The following steps of the algorithm can be distinguished:

1. Taking the data of the CUT and measurement results. Firstly, data describing the CUT are introduced: *N* – number of elements, $p_{i\,nom}$ - nominal values of parameters, analytical description of node functions (formulated in pretesting stage as Matlab function codes), which are used to real time computing the appropriate points representing p_i-loci. Next, the measurement frequency f_m and the results of measurements of real and imaginary part of node functions are collected.
2. Checking the distance between the nominal point and the measurement point. If the distance is less then an assumed value ε, the circuit is qualified as fault free and the algorithm is stopped. Otherwise, go to the next step.
3. Determination of minimum distances between the measurement point and each p_i-locus as well as of p_{iS}-values corresponding to the minimum distances.
4. Finding a p_i-locus nearest to the measurement point. Its index locates the faulty element, and its p_{iS}-value identifies a soft fault: $\Delta p_i = p_{i0} - p_{iS}$.

The procedure of step 3 is repeated *NS* times, where: *S* – number of iteration steps. For *s*=1 (*s*=1,2,..,*S*) the algorithm generates (calculates) L_1 points representing p_i-locus. For next values of index *s* the L_s points are generated around the minimum distance to previously determined point p_{is}, with the adequately smaller step. We assumed $L_1 = L_2 = .. = L_S = L$. In a practice we use *S*=3 and *L*=20. It gives *SL*=60 calculations in the process of determination of minimum distances between the measurement point and each p_i-locus. For the investigated 3-order low pass filter, with *N*=6 components, the number of all calculations *NSL*=360. Thus, the numerical complexity of the algorithm is moderate.

4.2. Multiple fault diagnosis algorithm

It is possible to extend the previous algorithm to multiple fault diagnosis by its generalisation. In this case the node circuit functions can be expressed as functions dependent on p_{i_1}, p_{i_2},.., p_{i_k} circuit parameters, where *k* – number of faults ($k \le 2m-1$ and $k \le N$).

The modified algorithm searches all $p_i p_l$-hypersurfaces for double fault diagnosis or all $p_{i_1} p_{i_2} .. p_{i_k}$-hypersolids for multiple fault diagnosis in 2*m*–dimensional space and finds a hypersurface or hypersolid lying nearest to the measurement point. Simultaneously it also finds $p_{iS_1} p_{iS_2} .. p_{iS_k}$-values with minimum distance to the measurement point. Steps of the algorithm:

1. Taking the data of the CUT and measurement results. Firstly, data describing the CUT are introduced: *N* – number of elements, $p_{i\,nom}$ - nominal values of parameters, analytical description of node functions of *k*-parameters, *k* –number of faults. Next, the measurement frequency f_m and the results of measurements of real and imaginary parts of node functions are collected.
2. Checking the distance between the nominal point and the measurement point. If the distance is less then an assumed value ε, the circuit is qualified as fault free and the algorithm is stopped. Otherwise, go to the next step.
3. Searching for minimum distance $d_{i_1 i_2 .. i_k S}$ between the measurement point and $p_{i_1} p_{i_2} .. p_{i_k}$ - hypersolids. This distance is determined in an iterative way, where *s* – index of iterating step (*s*=1,2,..,*S*). Around the point with minimum distance $d_{i_1 i_2 .. i_k s}$ are generated nodes of the lattice representing $p_{i_1} p_{i_2} .. p_{i_k}$ - hypersolids with smaller node distances in successive steps of iteration *s*.

4. Repeating step 3 for all hypersolids. The number of step repetitions is equal to k combinations from N elements C^N_k.
5. Determination of a minimum value d_{min} of the set of $d_{i_1 i_2 .. i_k S}$ values. It indicates a $p_{i_1} p_{i_2} .. p_{i_k}$ - hypersolid lying nearest the measurement point. Indexes of this hypersolid locate the faulty elements, and $p_{iS_1} p_{iS_2} .. p_{iS_k}$ -values corresponding to the minimum distance identifying faults.

We generate L^k points representing the $p_{i_1} p_{i_2} .. p_{i_k}$ - hypersolid. It gives SL^k calculations of distances between the measurement point and each $p_{i_1} p_{i_2} .. p_{i_k}$ - hypersolid. In this case, the number of all calculations of distances is equal to $SL^k\ C^N_k$. This algorithm needs $(L^{k-1}\ C^N_k)/N$ times more calculations than the algorithm for a single fault.

5. VERIFICATION OF THE 4D METHOD

The 4D method in single-fault version was experimentally verified and compared with the 2D method on example of the 3rd-order low-pass filter [4]. The circuit functions (Y_{in} for the 2D method and, K_u, Y_{in} for the 4D method) were measured by the transmittance analyser HP4192A. Measurements were carried out for each component change in the range from $0.7\ p_{i\ nom}$ to $2\ p_{i\ nom}$. Different soft faults of each p_i-parameter were physically entered to the CUT and diagnosed on the level of fault localisation and identification.

Example of experimental results is shown in the Table 1. It only concerns of results of localisation and identification of R_2 deviations from the nominal value.

Table 1. Relative errors of fault identification for R_2 resistor for the 2D and 4D methods

$p_i/p_{i\,nom}$	0.7	0.8	0.9	1.1	1.3	1.5	2
δ_{2D}	5,02	**C1**	3.43	2.65	**C1**	1.57	1.03
δ_{4D}	1,68	1.71	1.63	1.43	1.21	1.18	1.08

The Table 1 shows relative errors of R_2 fault identification in percent for the 2D method (δ_{2D}) and for the 4D method (δ_{4D}). Cases of false diagnostic results concerning the 2D methods are indicated in the table by a symbol of the element qualified as faulty.

It is seen from the Table 1 that the 4D method for all parameter deviations gives correct results of fault localisation and better identification accuracy of R_2-deviations. In the 2D method the false fault localisation appears two times. Complete results of verification of the 4D method for all elements of the CUT are included in a PhD dissertation [4]. They are similar and they confirm advantage the 4D method over the 2D one.

6. IMPLEMENTATION OF THE 4D AND 6D METHOD IN NEURAL NETWORKS

One of field of application of the considered methods are neural networks. Therefore different methods were implemented by us in neural networks and compared.

The 4D and 6D methods were implemented in the network of 3rd-layer perceptron type and investigated on the example of the 3rd-order low-pass Butterworth filter (consisting of 6 elements: 3 resistors and 3 capacitors) and compared with the 2D method. For the 2D method as a circuit function the input admittance Y_{in} was used. For both the 4D and 6D methods the same circuit functions were used: K_u – the voltage transmittance, Y_{in} – the input admittance and additionally for the 6D method K_{iu} – the current-voltage transmittance.

The neural networks were simulated in Matlab. All networks were designed for localisation of soft faults in the range $0.1p_{i\ nom}$ to $10p_{i\ nom}$ around the nominal state of CUT. We assumed that the circuit is faulty if the value of any p_i-element is outside the range of $0.9p_{i\ nom}$ to $1.1p_{i\ nom}$ ($|\Delta p_i| \geq 0.1 p_i$).

Binary coding of a faulty component has been applied. Talking into account, that CUT has only 6 elements, we used in the output layer 3 neurones for all investigated networks and the fault code: 000 – no fault, 001 – faulty R1, etc. The number of neurones in the input layer of the particular network was adequate to the dimension of the space: 2, 4 and 6.

The architectures of hidden layers were chosen in result of training and testing many configurations of networks with different number of neurones in two hidden layers. The training set was collected from 8 points from each of p_i-loci (for 0.1; 0.3; 0.5; 0.7; 2; 5; 7; 10 $p_{i\,nom}$). Including the nominal point it gives 49 elements of the set. The testing set was chosen similarly for other p_i-values. It had the same number of elements, but different in comparison with the training set.

The most important criterion of choosing the best architecture of the neural network was the minimal number of false decisions in the testing stage and minimal training time.

For the 2D method after training and testing 30 different configurations, the network, with 20 neurones in the first hidden layer and 15 neurones in the second one was chosen. This network for 49 tests makes 7 localisation errors. Hence, the fault localisation coverage (FLC – the number of good decisions of the neural network to the number of tests, describing the probability of correct fault localisation in percent) is equal to 85,7%. The training time is long and takes 1 hour and 14 minutes.

For finding the best architectures of the neural networks for the 4D and 6D methods, training and testing were made for 30 networks with different numbers of neurones in first and second hidden layer. The results are included in Table 2. Its columns are divided with regard to the number of neurones in first hidden layer (L1), and rows with regard to the number of neurones in second hidden layer (L2). In the first row of each cell are results of the network for the 4D method, in the second one the results for the 6D method. Each row of respective cells of the Table 2 contains the number of false decisions of the network divided by training time in minutes.

From the Table 2 it is seen that the best architecture of the network for the 4D method consists of 20 neurones in the first and 10 in the second hidden layer. For it the FLC is equal to 96% (2 mistakes in 49 tests) and the training time is less than 7 minutes.

Table 2. Results of training and testing the neural network for the 4D and 6D method, where L1 – the number of neurones in the first hidden layer, L2 – the number of neurones in the second hidden layer. First row of each cell represents results (number of false decisions / training time in minutes) for the 4D method, the second row the same for the 6D method.

L2: \ L1:		10	15	20	25	30
10	4D	2 / 11.5	4 / 11.1	**2 / 6.8**	4 / 17.3	3 / 8.9
	6D	4 / 6.4	2 /5.6	4 / 4.9	3 / 6.3	5 / 6.6
13	4D	4 / 7	6 / 4.3	3 / 5.5	7 / 11.6	6 / 5.5
	6D	**1 / 5.2**	4 / 3.8	2 / 10	4 / 4.1	5 / 5.9
15	4D	5 / 7.7	3 / 4.3	8 / 6.9	5 / 6.6	3 / 5.9
	6D	2 / 3	4 / 5.3	1 / 6.3	4 / 3.4	4 / 4
20	4D	5 / 6.6	3 / 6.9	3 / 5.4	4 / 7.4	6 / 12.3
	6D	2 / 4	4 / 5	4 / 3.7	3 / 3.2	4 / 5.7
23	4D	4 / 6.7	5 / 5.4	3 / 6.4	4 / 6.6	4 / 9.8
	6D	5 / 4.9	4 / 5.2	5 / 5	3 / 6.3	4 / 5
25	4D	4 / 10.4	6 / 6.9	7 / 6.6	7 / 9.8	5 / 9.2
	6D	5 / 6.3	6 / 6.9	4 / 5.9	5 / 4.5	6 / 6.9

For the 6D method we choose the network with 10 neurones in the first hidden layer and 13 in the second one because its architecture is simpler and it takes shorter training time (see Table 2). It makes only 1 mistake in 49 tests, what gives the FLC equal to 98% and training time of about 5 minutes.

The neural networks based on the 4D method (with FLC=96% and training time 6.8 minutes) and on the 6D method (with FLC=98% and time 5.2 minutes) have advantage over the 2D neural network (with FLC=85.7% and training time 1h and 14min). The 6D network is better in comparison with the 4D network and simpler. It has a lower number of neurones in hidden layers. Both the 4D and 6D neural networks can be applied to single fault localisation in electronic circuits and in monitoring other multi-parameter objects modelled by electrical circuits.

7. FIELDS OF POSSIBLE APPLICATIONS OF THE METHODS

Presented methods and algorithms, particularly in single and double-fault version, can be used to fault diagnosis of analogue electronic circuits and implemented in testing systems of printed circuit boards as part of method libraries. The are suitable for applications in testing with the aid of the mixed signal testing bus IEEE 1149.4, particularly for testing and diagnosis of circuits connecting VLSI chips.

These methods can be also used for parameter-identification measurements of multi-parameter objects modelled by electrical circuits, e.g. measurement transducers, anticorrosion coatings etc. Such objects are modelled by equivalent circuits with many elements (order 4 – 10) but only 1 or 2 element parameters are dependent on the measurement value. A good example is a humidity transducer with a porous aluminium oxide sensor. The equivalent circuit of the sensor consists of 7 R C elements, but only 2 element parameters are strongly dependent on humidity. In this case, for monitoring humidity the 3D or 4D algorithm in version limited to one p_i p_l-surface or hypersurface can be used.

8. CONCLUSIONS

Methods presented in the paper in two-port and in multiport versions based on proposed transformations in 3D, 4D, 6D and more dimensional spaces of circuits functions (input-output or node functions) may be useful for diagnosis of analogue electronic circuits on the level of localisation and identification of single, double and multiple faults. Essential feature of the methods is the location p_i-loci in multi-dimensional spaces which gives greater distances between the loci and enables significant increase of fault localisation resolution and accuracy of parameter identification. It also increases robustness against the DUT component tolerances and voltage measurement uncertainties.

The methods can be applied in practice to parametric fault diagnosis of analogue electronic circuits, as equipment of methodological libraries of in-circuit PCB testing systems and testers equipped in the mixed signal testing bus IEEE 1149.4. They can be useful in parameter-identification measurements of multi-parameter objects (order 10) modelled by electrical circuits. The methods can be also implemented in neural networks for parameter monitoring and classification.

REFERENCES

[1] Czaja Z., Zielonko R., *Fault diagnosis in electronic circuits based on bilinear transformation in 3D and 4D space*, In Proceedings of the IEEE on Instrumentation and Measurement, Technology Conference, Budapest, Hungary, May 21-23, 2001, Vol. 1, pp. 55-58.

[2] Czaja Z., Zielonko R., *New methods of fault diagnosis in electronic circuits based on bilinear transformation in multidimensional spaces*", Metrology and Measurement Systems, Vol. VIII. Number 3 (2001), Polish Scientific Publishers PWN Warsaw 2001, s. 251-262.

[3] Martens G., Dyck J., *Fault identification in electronic circuit with the aid of bilinear transformation*, IEEE Trans. on Reliability, No2, May 1972, pp.99-104.

[4] Czaja Z., *Input-output diagnosis of analogue electronic circuits based on the bilinear transformation*, PhD Thesis, in Polish, Gdansk University of Technology, Faculty of ET and I, Gdansk, 23 October 2001.

Author: Dr Zbigniew Czaja, Gdansk University of Technology, Faculty of Electronics, Telecommunications and Informatics, Department of Electronic Measurements, ul. G. Narutowicza 11/12, 80-952 Gdansk, Poland, phone ++48 58 347-14-87, fax ++48 58 347-22-55 and e-mail. zbczaja@pg.gda.pl

Author: Prof. Romuald Zielonko, Gdansk University of Technology, Faculty of Electronics, Telecommunications and Informatics, Department of Electronic Measurements, ul. G. Narutowicza 11/12, 80-952 Gdansk, Poland, phone ++48 58 347-22-55, fax ++48 58 347-22-55 and e-mail. zielonko@eti.pg.gda.pl